MODES IN A HARD SURFACE WAVEGUIDE WITH UNIAXIALLY ANISOTROPIC CHIRAL MATERIAL FILLING

S. F. Mahmoud

Electrical Engineering Department
Kuwait University, Kuwait

A. J. Viitanen

Electromagnetics Laboratory
Department of Electrical and Communications Engineering
Helsinki University of Technology
P.O. Box 3000, FIN-02015 HUT, Finland

Abstract—Propagation of waves in circular waveguide with the boundary condition of hard surface is considered. The waveguide is filled with uniaxial chiral material. This study is a generalization of previously studied cases with isotropic chiral or anisotropic material filling. The eigenvalue equation is formed and the corresponding eigenmodes are presented. It is seen that the hard surface boundary condition simplifies the field analysis remarkable. While the eigenwaves in anisotropic waveguide were TE and TM fields in this more general case the eigenwaves are elliptically polarized hybrid fields. Since the eigenwaves are certain combinations of TE and TM fields and propagate with different propagation factors, uniaxial chiral medium can be used for polarization transformation. Reflection and transmission from a uniaxial chiral section of a waveguide is analyzed with numerical examples.

1. INTRODUCTION

Corrugated waveguides are used in many applications for microwave engineering and a lot of research for corrugated surfaces and waveguides are done [1, 2]. Usually, the corrugation is in transverse direction. In this study the corrugations are made in the axial direction resulting in a waveguide with longitudinally slotted wall as introduced in [3]. The boundary conditions at the longitudinal slots dictate zero longitudinal electric field just as on a perfectly conducting wall. A similar boundary condition on the longitudinal magnetic field can also be imposed over a finite bandwidth if the slots are filled with a suitable dielectric material and the slot depth is adjusted to provide a 90 degrees radial phase shift [4]. This forms what has been termed as the hard surface boundary condition [5, 6]. This kind of special boundary condition is useful in many applications. In such a waveguide, there can propagate TE, TM and hybrid modes, even TEM waves , e.g., [4, 6]. Recently hard surface waveguide with anisotropic material filling, for example sapphire, was considered and shown to have a practical application as a polarization transformer [7]. Chiral material in such waveguide was analyzed in [8], where it was demonstrated that a hard surface waveguide section filled with slightly chiral material works as a dual mode transformer changing TE field to TM field or vice versa. In this study properties of fields in uniaxial chiral material propagating in a hard surface waveguide are considered. First, the propagating eigenmodes are given, then reflection and transmission at the interface of isotropic and uniaxial chiral waveguide are studied. By using the method given in [9] the reflected and transmitted fields are solved in the presence of a section of uniaxially anisotropic chiral material filling.

2. THEORY

We consider time harmonic fields ($e^{i\omega t}$) in a circular waveguide with hard surface (HS) at the radius $\rho = a$. The guide is filled with a homogeneous chiral material, but uniaxially anisotropic such that its

constitutive relations are [10]:

$$\mathbf{D} = \left[\epsilon_t \overline{\overline{I}}_t + \epsilon_z \mathbf{u}_z \mathbf{u}_z\right] \cdot \mathbf{E} - j\kappa\sqrt{\epsilon_z \mu_z}\mathbf{u}_z \mathbf{u}_z \cdot \mathbf{H} \tag{1}$$

$$\mathbf{B} = \left[\mu_t \overline{\overline{I}}_t + \mu_z \mathbf{u}_z \mathbf{u}_z\right] \cdot \mathbf{H} + j\kappa\sqrt{\epsilon_z \mu_z}\mathbf{u}_z \mathbf{u}_z \cdot \mathbf{E} \tag{2}$$

where κ is the chirality factor and $\mathbf{u}_z$ is a unit vector along the guide axis. To obtain the natural modes of propagation in the guide, we solve the source free Maxwell's equations. To this end, let us express the modal fields as transverse plus longitudinal components [11];

$$\mathbf{E} = (\mathbf{e} + E_z \mathbf{u}_z)e^{-j\beta z} \tag{3}$$

$$\mathbf{H} = (\mathbf{h} + H_z \mathbf{u}_z)e^{-j\beta z} \tag{4}$$

Applying Maxwell's two equations to the above modal fields, and separating the transverse and longitudinal components, we get the following four equations:

$$\nabla_t \times \mathbf{e} = -j\omega\left(\mu_z H_z + j\kappa\sqrt{\epsilon_z \mu_z}E_z\right)\mathbf{u}_z \tag{5}$$

$$\nabla_t \times \mathbf{h} = j\omega\left(\epsilon_z E_z - j\kappa\sqrt{\epsilon_z \mu_z}H_z\right)\mathbf{u}_z \tag{6}$$

$$-j\beta\mathbf{u}_z \times \mathbf{e} - \mathbf{u}_z \times \nabla_t E_z = -j\omega\mu_t\mathbf{h} \tag{7}$$

$$-j\beta\mathbf{u}_z \times \mathbf{h} - \mathbf{u}_z \times \nabla_t H_z = j\omega\epsilon_t\mathbf{e} \tag{8}$$

From (7) and (8), we can express the transverse fields in terms of their longitudinal counterparts in the usual manner

$$\mathbf{e} = -j\frac{\beta}{\lambda^2}\nabla_t E_z - j\frac{\omega\mu_t}{\lambda^2}\nabla_t H_z \times \mathbf{u}_z \tag{9}$$

$$\mathbf{h} = -j\frac{\beta}{\lambda^2}\nabla_t H_z - j\frac{\omega\epsilon_t}{\lambda^2}\mathbf{u}_z \times \nabla_t E_z \tag{10}$$

where $\lambda^2 = k_t^2 - \beta^2 = \omega^2\mu_t\epsilon_t - \beta^2$.

Now, using (9) and (10) in (5) and (6), and noting that $\nabla_t \times \nabla_t \psi = 0$, and $\nabla_t \times (\mathbf{u_z} \times \nabla_t \psi) = \mathbf{u}_z \nabla_t^2 \psi$, we get the wave equations for the longitudinal fields as:

$$\begin{bmatrix} \nabla_t^2 E_z \\ \nabla_t^2 H_z \end{bmatrix} + \lambda^2 \begin{bmatrix} \epsilon_z/\epsilon_t & -j\kappa\sqrt{\epsilon_z \mu_z}/\epsilon_t \\ j\kappa\sqrt{\epsilon_z \mu_z}/\mu_t & \mu_z/\mu_t \end{bmatrix} \begin{bmatrix} E_z \\ H_z \end{bmatrix} = 0 \tag{11}$$

which shows that, as expected, the two longitudinal fields are coupled by the chirality. So, the fields are generally hybrid, instead of being TE or TM as in the case of zero chirality [7]. One can obtain the modal

field structure by finding the eigenvectors and eigenvalues of the 2×2 matrix in (11). Denoting the eigenvalues by k_c^2, we get:

$$k_c^2 = \frac{\lambda^2}{2} \left[\frac{\epsilon_z}{\epsilon_t} + \frac{\mu_z}{\mu_t} \pm \sqrt{\left(\frac{\epsilon_z}{\epsilon_t} - \frac{\mu_z}{\mu_t} \right)^2 + 4\kappa^2 \frac{\epsilon_z \mu_z}{\epsilon_t \mu_t}} \right] \quad (12)$$

The corresponding eigenfunctions determine the hybrid nature of the modes and are given by:

$$(E_z, H_z) = \left(E_z, \; j\sqrt{\epsilon_t/\mu_t}\, \Lambda^{-1} E_z \right) \quad (13)$$

where

$$\Lambda^{-1} = \left(\frac{k_c^2}{\lambda^2} - \frac{\epsilon_z}{\epsilon_t} \right) \frac{\sqrt{\mu_t \epsilon_t / \mu_z \epsilon_z}}{\kappa} \quad (14)$$

is the mode hybrid factor.

As a checking special case, if the medium is isotropic, with a uniaxial chirality; i.e. $\epsilon_z = \epsilon_t$, $\mu_z = \mu_t$, (12) and (14) reduce to: $k_c^2 = \lambda^2(1 \pm \kappa)$ and $\Lambda = \pm 1$, corresponding to right and left circularly polarized modes as expected, [8]. On the other hand if the chirality is zero, (12) and (14) reduce to: $k_c^2 = \lambda^2 \epsilon_z/\epsilon_t$ along with $\Lambda = \infty$ for TM modes, and $k_c^2 = \lambda^2 \mu_z/\mu_t$ along with $\Lambda = 0$ for TE modes in agreement with [7].

Now consider the boundary conditions at the wall $\rho = a$ of the circular waveguide. Because of the HS, these require that both $E_z = 0$ and $H_z = 0$. Hence, in view of the wave equation, each of these two fields will have the form: $\psi(\rho, \varphi) = J_n(k_c \rho)e^{-jn\varphi}$. Application of the boundary conditions immediately sets $k_c = p_{ns}/a$. Here p_{ns} is the sth root of the $J_n(\cdot)$. Now using (12), we get two values for β for each pair n and s. These correspond to two hybrid modes with different hybrid factor and polarization state as will be shown next. The propagation factors and the corresponding hybrid factors are:

$$\beta_\pm^2 = k_t^2 - \frac{p_{ns}^2/a^2}{2(1-\kappa^2)} \frac{\epsilon_t \mu_t}{\epsilon_z \mu_z} \left[\frac{\epsilon_z}{\epsilon_t} + \frac{\mu_z}{\mu_t} \mp \sqrt{\left(\frac{\epsilon_z}{\epsilon_t} - \frac{\mu_z}{\mu_t} \right)^2 + 4\kappa^2 \frac{\epsilon_z \mu_z}{\epsilon_t \mu_t}} \right], \quad (15)$$

$$\Lambda_\pm = \pm \frac{\sqrt{\epsilon_t \mu_t}}{2\kappa\sqrt{\epsilon_z \mu_z}} \left[\sqrt{\left(\frac{\epsilon_z}{\epsilon_t} - \frac{\mu_z}{\mu_t} \right)^2 + 4\kappa^2 \frac{\epsilon_z \mu_z}{\epsilon_t \mu_t}} \pm \left(\frac{\epsilon_z}{\epsilon_t} - \frac{\mu_z}{\mu_t} \right) \right] \quad (16)$$

It is interesting to notice here that $\Lambda_+ \Lambda_- = -1$. So, the hybrid factors of the two modes have opposite signs and magnitudes higher and lower than unity. This is related to the polarization of the eigenfields. These
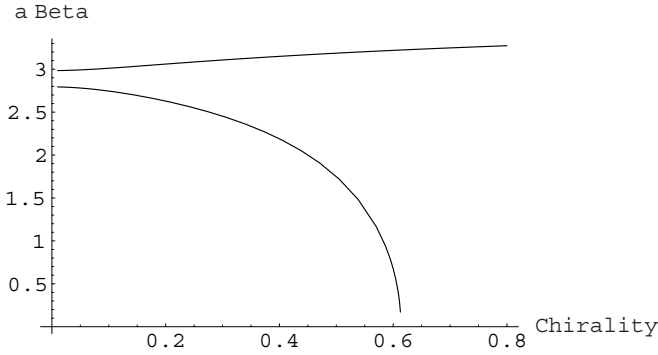
Figure 1. Propagation factors for $+$ and $-$ fields as a function of the chirality factor, for $k_o = k_c/2$, $\epsilon_t = 9.4$, $\epsilon_z = 11.6$, $\mu_t = \mu_z = 1$ and $k_c = p_{01}/a$.

$+$ and $-$ eigenfields are elliptically polarized with opposite handedness. As a numerical example, the normalized propagation factors $\beta_{\pm}a$ are plotted versus the chirality parameter κ in Figure 1 for the given medium parameters. It is seen that one of the eigenwaves has a cutoff at high values of chirality.

3. EIGENFIELDS

The eigenfields, denoted by $+$ and $-$ waves are propagating separately, or uncoupled, with different propagation factors. Hence the polarization of the total field is changed. This contrasts the case of isotropic waveguide where the propagation factors are the same for both eigenfields (TE and TM), hence the polarization remains unchanged. It is convenient to denote the hybrid factor as $\Lambda_+ = \Lambda$ and $\Lambda_- = -1/\Lambda$ where

$$\Lambda = \frac{\sqrt{\epsilon_t \mu_t}}{2\kappa \sqrt{\epsilon_z \mu_z}} \left[\sqrt{\left(\frac{\epsilon_z}{\epsilon_t} - \frac{\mu_z}{\mu_t}\right)^2 + 4\kappa^2 \frac{\epsilon_z \mu_z}{\epsilon_t \mu_t}} + \left(\frac{\epsilon_z}{\epsilon_t} - \frac{\mu_z}{\mu_t}\right) \right] \qquad (17)$$

The eigenfields are given by (13) and we can explicitly write

$$E_{z\pm}(\rho, \varphi, z) = \frac{E_{\pm} \psi(\rho, \varphi)}{\sqrt{N_{\pm}}} e^{-j\beta_{\pm} z} \qquad (18)$$

where $E_{\pm}$ are eigenwave amplitudes, and $N_{\pm}$ are normalizing factors to be chosen such that the powers associated with the transverse fields

of the $+$ and $-$ waves are equal to unity when $E_\pm = 1$. Denoting the transverse vector $\mathbf{u} = \nabla_t \psi$, the transverse fields associated with the longitudinal field in (18) are:

$$\mathbf{e}_+ = \frac{E_+ e^{-j\beta_+ z}}{\lambda_+^2 \sqrt{N_+}} [-j\beta_+ \mathbf{u} - \frac{k_t}{\Lambda} \mathbf{u}_z \times \mathbf{u}], \quad \mathbf{e}_- = \frac{E_- e^{-j\beta_- z}}{\lambda_-^2 \sqrt{N_-}} [-j\beta_- \mathbf{u} + k_t \Lambda \mathbf{u}_z \times \mathbf{u}]$$
(19)

$$\mathbf{h}_+ = \frac{E_+ e^{-j\beta_+ z}}{\lambda_+^2 \eta_t \sqrt{N_+}} [\frac{\beta_+}{\Lambda} \mathbf{u} - j k_t \mathbf{u}_z \times \mathbf{u}], \quad \mathbf{h}_- = \frac{E_- e^{-j\beta_- z}}{\lambda_-^2 \eta_t \sqrt{N_-}} [-\beta_- \Lambda \mathbf{u} - j k_t \mathbf{u}_z \times \mathbf{u}]$$
(20)

where $\eta_t = \sqrt{\mu_t/\epsilon_t}$ and $\lambda_\pm^2 = k_t^2 - \beta_\pm^2$. For normalization to a unit power of the $+$ and $-$ eigenwaves per unit $E_\pm$, we choose $N_\pm$ as

$$N_\pm = \frac{k_t \beta_\pm}{\lambda_\pm^4 \eta_t} \left(1 + \frac{1}{\Lambda^2} \right)$$
(21)

The wave impedances for the transverse eigenfields are

$$\mathbf{e}_\pm = \overline{\overline{Z}}_\pm \cdot \mathbf{h}_\pm$$
(22)

where

$$\overline{\overline{Z}}_+ = -j\eta_t \left[\Lambda \mathbf{u}\mathbf{u} + \frac{1}{\Lambda} (\mathbf{u}_z \times \mathbf{u})(\mathbf{u}_z \times \mathbf{u}) \right],$$
$$\overline{\overline{Z}}_- = j\eta_t \left[\frac{1}{\Lambda} \mathbf{u}\mathbf{u} + \Lambda (\mathbf{u}_z \times \mathbf{u})(\mathbf{u}_z \times \mathbf{u}) \right]$$
(23)

which obey the relation $\overline{\overline{Z}}_+ \cdot \overline{\overline{Z}}_- = \eta_t^2 \overline{\overline{I}}_t$. For isotropic medium, $\Lambda = 1$, the wave impedances are

$$\overline{\overline{Z}}_\pm = \mp j\eta \overline{\overline{I}}_t$$
(24)

For example, to study the mode polarization state, let us concentrate on the two dominant modes corresponding to $n = 0$ and $s = 1$. The boundary condition of HS is equal to $J_0(k_c a) = 0$ with $k_c = p_{01}/a$ in which case $p_{01} = 2.4048$. The transverse electric eigenfields are obtained by using equations (9) and (13), and take the form:

$$\mathbf{e}_\pm = \frac{j\beta_\pm p_{01}/a E_\pm}{\lambda_\pm^2 \sqrt{N_\pm}} J_1 \left(\frac{p_{01}\rho}{a} \right) \left[\mathbf{u}_\rho - j \frac{k_t}{\Lambda_\pm \beta_\pm} \mathbf{u}_\varphi \right]$$
(25)

Calculating the helicity vector $\mathbf{p} = p_\pm \mathbf{u}_z$, as defined by Lindell [12], we get:

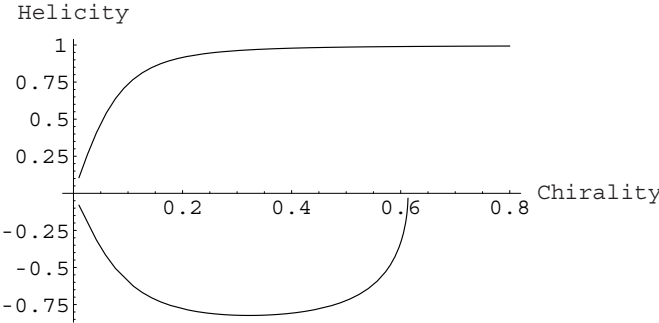$$p_\pm = \frac{2k_t/\Lambda_\pm \beta_\pm}{1 + (k_t/\Lambda_\pm \beta_\pm)^2}$$
(26)

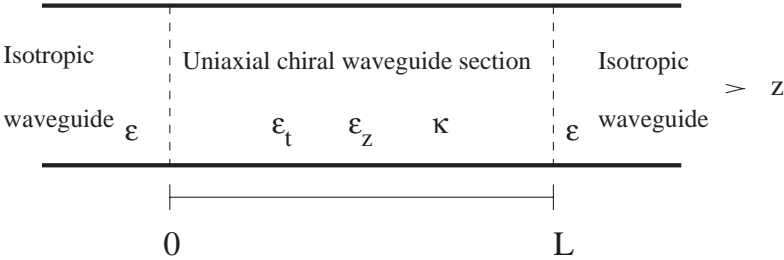**Figure 2.** Helicity factor for transverse electric eigenfields; + wave (upper curve) and − wave (lower curve).

Figure 3. A uniaxial chiral waveguide section between two isotropic guides.

Note that the hybrid factor $\Lambda_\pm$ changes sign from one mode to the other; hence the two modes are generally of opposite elliptical polarization as shown in Figure 2.

In [7] it was found that the polarization of the transverse fields is changed with anisotropic material filling only when there are both TE and TM fields present, and the maximum change in polarization is proportional to the ratio of axial electric and magnetic field components. In this chiral anisotropic case also the ratio of the axial field components changes but the polarization transformation occurs even in the case when we have either TE or TM incident field. By inserting chirality in anisotropic material one can transform, for example, the incident transverse TM field, which is linearly polarized, to circularly polarized field.

4. REFLECTION AND TRANSMISSION AT ISOTROPIC AND ANISOTROPIC CHIRAL INTERFACE

Let us consider the reflection and transmission at the interface between isotropic hard surface waveguide and anisotropic chiral hard surface waveguide having the same radius as shown in Figure 3. It is important to note that, because of the nature of a hard surface boundary conditions, an incident mode of order (n, s) from any side of the interface will excite modes of only the same order (n, s). This is so since the transverse field distribution over the waveguide cross-section is the same on both sides of the interface provided that the radius of the waveguide does not change. So, the problem of scattering at the interface reduces to a transmission line junction with two modes on each side. Now, since the modal fields inside isotropic waveguide on the left hand of the interface $z = 0$ are TE and TM fields and propagating with the same propagation factor $\beta = \sqrt{k^2 - k_c^2}$, the incident and reflected waves are written in terms of TE and TM waves. The transverse fields consist of incident and reflected parts:

$$
\begin{aligned}
\sqrt{N}\,\mathbf{e}_1 \;=\; & -j\frac{\beta}{k_c^2}E^i e^{-j\beta z}\mathbf{u} + j\frac{k\eta}{k_c^2}H^i e^{-j\beta z}\mathbf{u}_z \times \mathbf{u} \\
& +j\frac{\beta}{k_c^2}E^r e^{j\beta z}\mathbf{u} + j\frac{k\eta}{k_c^2}H^r e^{j\beta z}\mathbf{u}_z \times \mathbf{u} \qquad (27)
\end{aligned}
$$

$$
\begin{aligned}
\sqrt{N}\,\mathbf{h}_1 \;=\; & -j\frac{k}{k_c^2\eta}E^i e^{-j\beta z}\mathbf{u}_z \times \mathbf{u} - j\frac{\beta}{k_c^2}H^i e^{-j\beta z}\mathbf{u} \\
& -j\frac{k}{k_c^2\eta}E^r e^{j\beta z}\mathbf{u}_z \times \mathbf{u} + j\frac{\beta}{k_c^2}H^r e^{j\beta z}\mathbf{u} \qquad (28)
\end{aligned}
$$

where $k = \omega\sqrt{\mu\epsilon}$, $\beta = \sqrt{k^2 - k_c^2}$, and $\eta = \sqrt{\mu/\epsilon}$. Again N is a normalizing factor such that a unit power is carried by the transverse fields when E^i, $E^r = 1$ or ηH^i, $\eta H^r = 1$, namely, $N = \beta k/k_c^4\eta$. In waveguide filled with uniaxial chiral medium, the electric and magnetic fields are expressed with the elliptically polarized modal fields (19) and (20) :

$$
\mathbf{e}_2 = \mathbf{e}_+ + \mathbf{e}_-, \qquad \mathbf{h}_2 = \mathbf{h}_+ + \mathbf{h}_- \qquad (29)
$$

The continuity of the transverse fields at the interface $z = 0$ are considered which straitforwardly leads to the expression for the reflection coefficients and transmission coefficients. The reflected axial field components are

$$
\begin{bmatrix} E^r \\ j\eta H^r \end{bmatrix} = \begin{bmatrix} R_{EE} & R_{EH} \\ R_{HE} & R_{HH} \end{bmatrix} \begin{bmatrix} E^i \\ j\eta H^i \end{bmatrix} \qquad (30)
$$

with the reflection coefficients

$$R_{EE} = \left[\left(1 + \frac{k\beta_-\eta}{k_t\beta\eta_t}\right)\left(1 - \frac{k\beta_+\eta_t}{k_t\beta\eta}\right) + \frac{1}{\Lambda^2}\left(1 + \frac{k\beta_+\eta}{k_t\beta\eta_t}\right)\left(1 - \frac{k\beta_-\eta_t}{k_t\beta\eta}\right)\right]\frac{1}{d} \tag{31}$$

$$R_{HH} = \left[\left(1 + \frac{k\beta_+\eta_t}{k_t\beta\eta}\right)\left(1 - \frac{k\beta_-\eta}{k_t\beta\eta_t}\right) + \frac{1}{\Lambda^2}\left(1 - \frac{k\beta_+\eta}{k_t\beta\eta_t}\right)\left(1 + \frac{k\beta_-\eta_t}{k_t\beta\eta}\right)\right]\frac{1}{d} \tag{32}$$

$$R_{EH} = R_{HE} = \left[2\frac{k}{k_t}\left(\frac{\beta_+ - \beta_-}{\beta}\right)\frac{1}{\Lambda}\right]\frac{1}{d} \tag{33}$$

with

$$d = \left(1 + \frac{k\beta_+\eta_t}{k_t\beta\eta}\right)\left(1 + \frac{k\beta_-\eta}{k_t\beta\eta_t}\right) + \frac{1}{\Lambda^2}\left(1 + \frac{k\beta_+\eta}{k_t\beta\eta_t}\right)\left(1 + \frac{k\beta_-\eta_t}{k_t\beta\eta}\right) \tag{34}$$

Using E_+ and E_- as transmitted axial field components of eigenmodes, and normalizing the modal fields on both sides of the junction to a unit power, we get

$$\left[\begin{array}{c} E_+ \\ E_- \end{array}\right] = \left[\begin{array}{cc} T_{+E} & T_{+H} \\ T_{-E} & T_{-H} \end{array}\right]\left[\begin{array}{c} E^i \\ j\eta H^i \end{array}\right] \tag{35}$$

where the transmission coefficients are

$$\left[\begin{array}{cc} T_{+E} & T_{+H} \\ T_{-E} & T_{-H} \end{array}\right] =$$

$$\left[\begin{array}{cc} K_+\left(\Lambda\frac{\eta_t}{\eta}(1 + R_{EE}) - R_{HE}\right) & K_+\left(\Lambda\frac{\eta_t}{\eta}R_{EH} - (1 + R_{HH})\right) \\ K_-\left(\frac{\eta_t}{\eta\Lambda}(1 + R_{EE}) + R_{HE}\right) & K_-\left(\frac{\eta_t}{\eta\Lambda}R_{EH} + (1 + R_{HH})\right) \end{array}\right] \tag{36}$$

with

$$K_+ = \sqrt{\frac{\eta\beta_+ k/\Lambda}{\eta_t\beta k_t(\Lambda + 1/\Lambda)}}, \quad K_- = \sqrt{\frac{\eta\beta_- k\Lambda}{\eta_t\beta k_t(\Lambda + 1/\Lambda)}}$$

It can be shown that the following power conservation relations hold:

$$R_{EE}^2 + R_{HE}^2 + T_{+E}^2 + T_{-E}^2 = 1 \quad (TM \text{ incident wave}) \tag{37}$$

$$R_{HH}^2 + R_{EH}^2 + T_{+H}^2 + T_{-H}^2 = 1 \quad (TE \text{ incident wave}) \tag{38}$$

It should be emphasized that the reflection coefficients are given between TE and TM fields, whereas the transmission coefficients give the transition from TE and TM fields to $+$ and $-$ modal fields. The reflection and transmission coefficients are illustrated in Figures 4 and
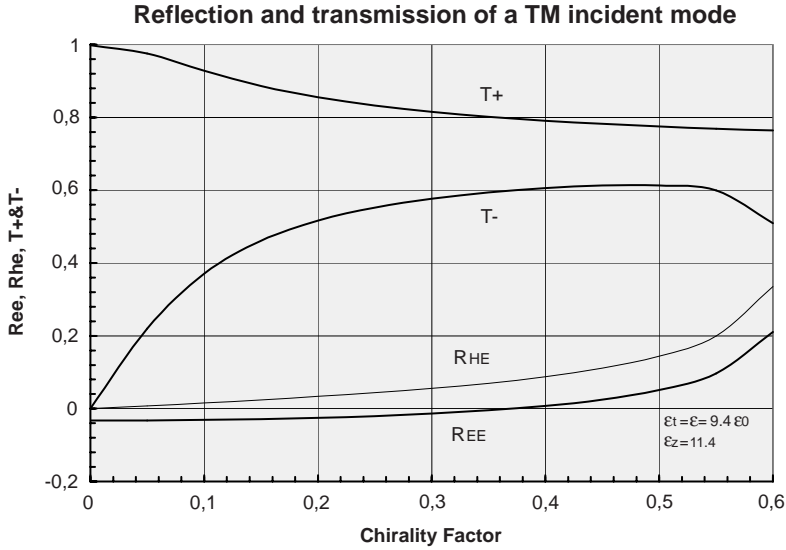
Reflection and transmission of a TM incident mode

Figure 4. Reflection and transmission factors, $\epsilon = \epsilon_t = 9.4\,\epsilon_o$ and $\epsilon_z = 11.6\,\epsilon_o$.

5 as a function of the chirality factor when the incident field is TM field with two different isotropic permittivity values; $\epsilon_r = 9$ and $\epsilon_r = 5$. It is seen that in both cases the reflection is quite small for values of κ up to 0.5. Namely, the reflection is less than 5 per cent for $\epsilon_r = 9$ and less than 14 per cent for $\epsilon_r = 5$.

5. SCATTERING FROM A UNIAXIAL CHIRAL WAVEGUIDE TO AN ISOTROPIC WAVEGUIDE WITH HS WALLS

Let the modes incident from the uniaxial chiral waveguide be characterized by amplitudes E_+ and E_-, normalized such that each mode carries unit power. At the junction with the isotropic waveguide, in Figure 3 at $z = L$, reflected and transmitted modes arise. Let the amplitude of the reflected modes be E_+^r and E_-^r and the transmitted modes be E^t and $j\eta H^t$, again normalized to a unit power. Working out the continuity of the tangential fields to the junction, we get:

$$\begin{bmatrix} E_+^r \\ E_-^r \end{bmatrix} = \begin{bmatrix} R_{++} & R_{+-} \\ R_{-+} & R_{--} \end{bmatrix} \begin{bmatrix} E_+ \\ E_- \end{bmatrix} \tag{39}$$
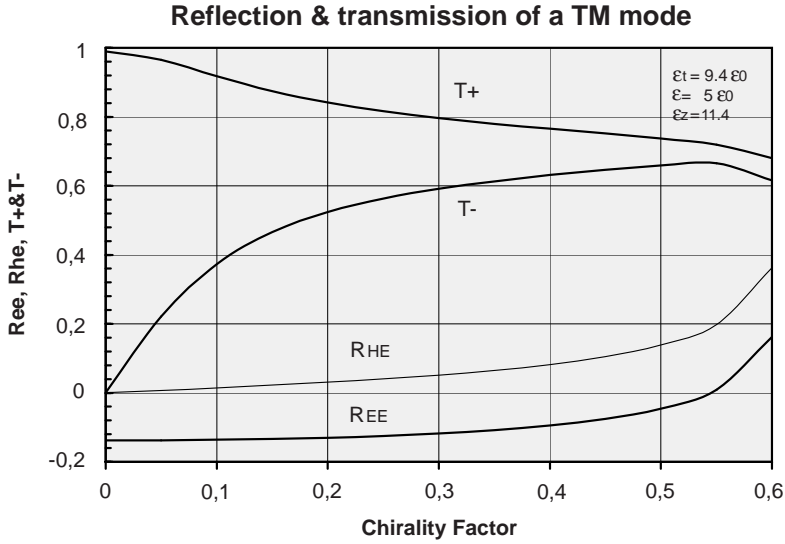
Reflection & transmission of a TM mode

Figure 5. Reflection and transmission factors, $\epsilon = 5\,\epsilon_o$, $\epsilon_t = 9.4\,\epsilon_o$ and $\epsilon_z = 11.6\,\epsilon_o$.

where

$$R_{++} = \left[\left(\frac{\beta_- k\eta}{\beta k_t \eta_t} + 1\right)\left(\frac{\beta_+ k\eta_t}{\beta k_t \eta} - 1\right) + \frac{1}{\Lambda^2}\left(\frac{\beta_- k\eta_t}{\beta k_t \eta} + 1\right)\left(\frac{\beta_+ k\eta}{\beta k_t \eta_t} - 1\right)\right]\frac{1}{d} \tag{40}$$

$$R_{--} = \left[\left(\frac{\beta_- k\eta}{\beta k_t \eta_t} - 1\right)\left(\frac{\beta_+ k\eta_t}{\beta k_t \eta} + 1\right) + \frac{1}{\Lambda^2}\left(\frac{\beta_- k\eta_t}{\beta k_t \eta} - 1\right)\left(\frac{\beta_+ k\eta}{\beta k_t \eta_t} + 1\right)\right]\frac{1}{d} \tag{41}$$

$$R_{+-} = R_{-+} = \frac{2}{d}\sqrt{\frac{\beta_+ \beta_-}{\beta^2}}\,\frac{k}{\Lambda k_t}\left(\frac{\eta_t}{\eta} - \frac{\eta}{\eta_t}\right) \tag{42}$$

The transmission matrix is defined by

$$\begin{bmatrix} E^t \\ j\eta H^t \end{bmatrix} = \begin{bmatrix} T_{E+} & T_{E-} \\ T_{H+} & T_{H-} \end{bmatrix}\begin{bmatrix} E_+ \\ E_- \end{bmatrix} \tag{43}$$

Comparing with the transmission coefficients defined by (36), numerical evaluations show that the following equalities are valid:

$$T_{E+} = T_{+E},\ T_{H-} = T_{-H},\ T_{E-} = T_{-E},\ T_{H+} = T_{+H}, \tag{44}$$

which reflects the validity of the reciprocity principle.

Now consider a section of uniaxial chiral waveguide of length L between two isotropic guides (see Figure 3). We wish to find the net reflection and transmission matrices between the terminal waveguides. To this end, let us define the following 2×2 matrices.

$$R_{i,u} \equiv \begin{bmatrix} R_{EE} & R_{EH} \\ R_{HE} & R_{HH} \end{bmatrix}, \quad R_{u,i} \equiv \begin{bmatrix} R_{++} & R_{+-} \\ R_{-+} & R_{--} \end{bmatrix},$$

$$\text{and} \ \ T_{i,u} \equiv \begin{bmatrix} T_{+E} & T_{+H} \\ T_{-E} & T_{-H} \end{bmatrix} \tag{45}$$

Note that the subscript (i, u) denotes the case of incidence from the isotropic guide to the uniaxial chiral guide. In contrast the subscript (u, i) denotes the opposite case of incidence from the uniaxial chiral guide to the isotropic one. Due to reciprocity, we can confirm that $T_{u,i} = T_{i,u}^T$, where the superscript T stands for the transpose operation. Now, considering an incident pair of modes from the input of the LHS isotropic guide, see Figure 3, and following the net reflection (out of the LHS guide) and transmission (out of the RHS guide) matrices as:

$$R_{net} = R_{i,u} + T_{u,i}(I - M)^{-1}DR_{u,i}DT_{i,u} \tag{46}$$

$$T_{net} = T_{u,i}(I - M^{-1})DT_{i,u} \tag{47}$$

where,

$$D = \begin{bmatrix} e^{-j\beta_+ L} & 0 \\ 0 & e^{-j\beta_- L} \end{bmatrix} \tag{48}$$

is the delay matrix through the uniaxial chiral section and I is the unit 2×2 matrix. The M matrix accounts for multiple reflections at the interfaces $z = 0$ and $z = L$. Namely

$$M = DR_{u,i}DR_{u,i} \tag{49}$$

It is worth mentioning that (46) and (47) are special cases of the problem treated recently by Uusitupa and Viitanen [9] where a nonreciprocal gyrotropic section is considered between two isotropic sections.

Numerical Examples:

We consider a unit incident power of linearly polarized TM wave to be incident from the left hand isotropic waveguide. In the absence of chirality; $\kappa = 0$, the uniaxial section of length L will not cause any conversion to the TE mode in the output waveguide since TM and TE modes propagate independently in such a guide. Hence the polarization will remain linear at the output. However with nonzero
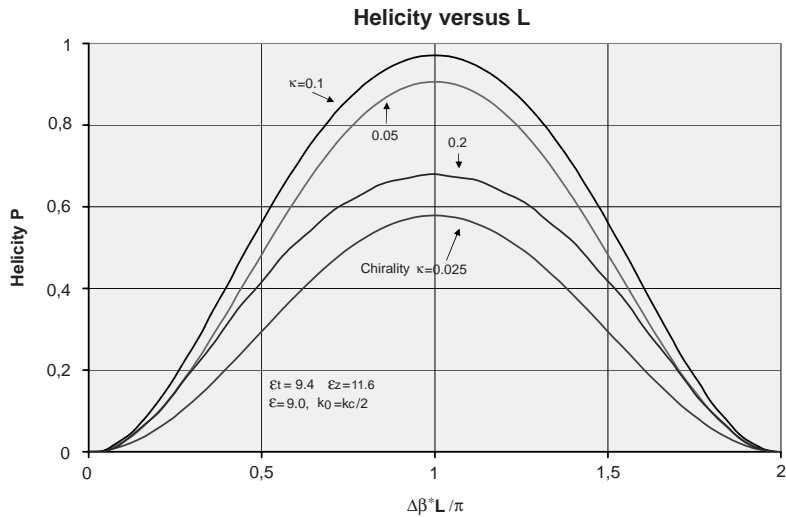
Helicity versus L

Figure 6. Helicity as a function of normalized length.
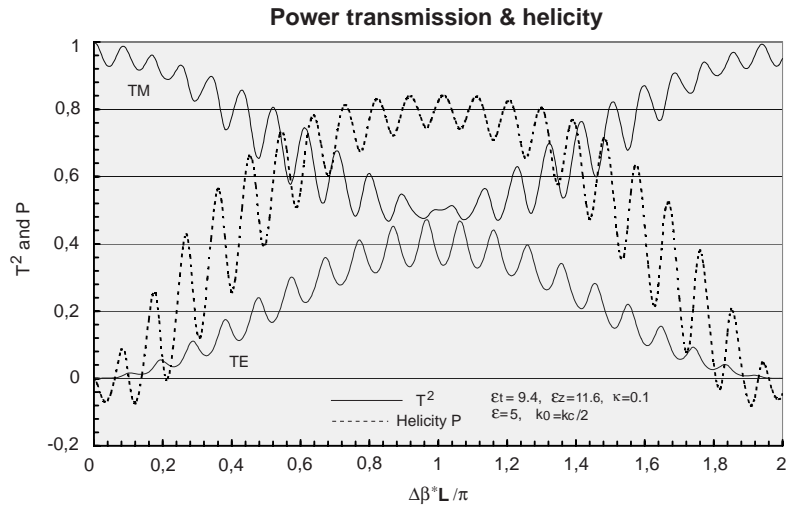
Power transmission & helicity

Figure 7. Power transmission factors and helicity as a function of normalized length, the relative chirality factor $\kappa = 0.1$.

chirality, continuous coupling between the modes occurs and causes TM/TE conversion at the output guide. It should be emphasized that axial chirality is sufficient for mode conversion. We show the helicity factor p in the output waveguide in Figure 6. The horizontal axis is the normalized length $\Delta\beta L/\pi = (\beta_+ - \beta_-)L/\pi$ and is taken between 0 and 2, while the chirality factor κ is a varying parameter. It is seen that for a given chirality, p attains a maximum at $\Delta\beta L/\pi = 1$. This maximum approaches unity (corresponding to circular polarization) at a given κ beyond which the maximum p decreases. While the permittivity of the isotropic sections $\epsilon = 9\,\epsilon_o$ is close to ϵ_t in Figure 6, it is reduced to $\epsilon = 5\,\epsilon_o$ in Figure 7. In this Figure we plot the power transmission factors in TM and TE modes as well as the helicity p for fixed chirality $\kappa = 0.1$. Because of the presence of significant reflection in this case, oscillations occur in the output transmission factors and helicity. Comparing these results with [7] it is shown in Figure 6 that having chirality in uniaxial anisotropic material the optimum polarization transformation (from linear to circular) is obtained with a certain chirality value. With sapphire (pure anisotropic material) this was not possible.

6. CONCLUSION

Having chirality in anisotropic material the difference between the propagation factors becomes greater than without chirality. This reduces the length of the waveguide section required for optimal polarization transformation which was found several wavelengths for sapphire filled waveguide. Also having chirality the transformation from either TM or TE field to circularly or elliptically polarized field is achieved which was not the case with anisotropic filling material. The ellipticity and the handedness of the polarization can be controlled by the medium parameters. For large values of the chirality parameter, one of the two eigenwaves has cut-off. The reflection and transmission in the interface of isotropic/chiral anisotropic waveguide is considered and the respective reflection and transmission coefficients are given. Also a waveguide section filled with anisotropic chiral material is considered with numerical examples which show clearly the effect of chirality. The hard surface boundary is here taken as an ideal boundary condition. However, in practice the hard surface boundary is realized with corrugation. This is quite narrow band behaviour. Actually, the ideal hard surface boundary condition is satisfied for both eigenwaves when the permittivity of the filling material inside the corrugation gaps is very high.

REFERENCES

1. Clarricoats, P. J. B. and A. D. Olver, *Corrugated Horns for Microwave Antennas*, Peregrinus, Stevenage, 1984.
2. Mahmoud, S. F., *Electromagnetic Waveguides; Theory and Applications*, Peregrinus Ltd., London, UK, 1991.
3. Scharten, T., J. Nellen, and V. D. Bogaart, "Longitudinally slotted conical horn antenna with small flare angle," *IEE Proceedings, Pt. H*, Vol. 128, 117–123, 1981.
4. Aly, M. S. and S. F. Mahmoud, "Propagation and radiation behavior of a longitudinally slotted horn with dielectric filled slots," *IEE Proceedings, Pt. H*, Vol. 132, 477–479, 1985.
5. Lier, E. and P-S. Kildal, "Soft and hard horn antennas," *IEEE Trans. Antennas Propagat.*, Vol. 36, 1152–1157, 1988.
6. Kildal, P-S., "Artificially soft and hard surfaces in electromagnetics," *IEEE Trans. Antennas Propagat.*, Vol. 38, No. 10, 1537–1544, October 1990.
7. Viitanen, A. J. and T. M. Uusitupa, "Fields in anisotropic hard-surface waveguide with application to polarization transformer," *IEE Proceedings, Microwaves, Antennas and Propagation*, Vol. 148, No. 5, 313–317, October 2001.
8. Viitanen, A. J., "Chiral hard surface mode transformer," *IEEE Trans. Microwave Theory and Techniques*, Vol. 48, No. 6, 1077–1079, June 2000.
9. Uusitupa, T. M. and A. J. Viitanen, "Analysis of finite-length gyrotropic hard-surface waveguide," *Radio Science*, to appear.
10. Lindell, I. V. and A. J. Viitanen, "Plane wave propagation in a uniaxial bianisotropic medium," *Electron. Lett.*, Vol. 29, No. 2, 150–152, 1993.
11. Collin, R. E., *Foundations for Microwave Engineering*, McGraw-Hill, New York, 1966.
12. Lindell, I. V., *Methods for Electromagnetic Field Analysis*, Clarendon Press, Oxford, 1992.